

mentary Table S1 and Figure S10).

Summary

An approach has been described for structural modelling of relatively small molecules by NMR. The first step involves setting up primary restraints to account for the covalent structure of the molecule of interest. For 12,13-diepi-F430, covalent angles and distances were derived from X-ray crystallographic data published for related coenzyme B₁₂ derivatives. In general, standard van der Waals radii were employed, with the exception that atoms of the five- and six-membered rings of the macrocycle were allowed to approach to distances less than the sums of their van der Waals radii in order to maximize conformational sampling. It is essential to utilize proper primary restraint parameters when extending algorithms designed for structural modelling of biopolymers to small molecules, and one must demonstrate that the primary restraints alone allow for sufficient conformational flexibility. Structures generated by our distance geometry approach using only primary restraints exhibited significant conformational diversity, with each of the unsaturated five-membered pyrrole units and the six-membered ring existing in several low-penalty conformations. Back-calculated NOESY spectra for these DG/SA structures were shown to deviate significantly compared to the experimental NOESY spectra.

Structures generated subsequently with the addition of "loose" NOE-derived distance restraints converged to a unique conformation, and the similarity of the back-calculated and experimental NOESY spectra indicates that the DG(+NOE) structures are reasonable representatives of the solution-state conformation of 12,13-diepi-F430. The DG(+NOE) structures compare favorably with the X-ray structure of 12,13-diepi-F430M, with pairwise RMSDs for the 24 macrocyclic ring atoms of ca. 0.28 Å. The DG(+NOE) and X-ray structures exhibit a similar corphin ring conformation that is characterized by an extreme saddle-shaped ring deformation, which was predicted on the basis of X-ray studies

of Ni(II)-containing hydrocorphinoid complexes.¹⁶⁻¹⁹

The NMR-based approach has several limitations; in particular, regardless of the quality of NMR data, the "resolution" of the NMR structures will certainly never approach the high resolution obtainable by X-ray diffraction techniques. In addition, the NMR approach relies intimately on knowledge of the primary structure, including atomic stereochemistry and electronic conjugation, and without full knowledge of these parameters the implementation of the NMR-based approach should be avoided. Nevertheless, for molecules that have proven difficult or impossible to crystallize, such as native F430, the NMR approach provides an attractive alternative for structural modelling. Applications to other small-molecule systems for which high-resolution X-ray structural results are available will establish the reliability and ultimate potential of this technique.

Acknowledgment. Financial support from the Petroleum Research Fund, administered by the American Chemical Society (to M.F.S.), NSF Grant DMB 86-13679 and NIH Grant AI12277 (to R.W.), and technical support from Bernie Duffy (UMBC), Victor Gabriel (UIUC), and Scott Smith (UIUC) are gratefully acknowledged. C.K. acknowledges support from the Austrian Science Foundation.

Registry No. 12,13-Diepimeric F430, 142186-78-5.

Supplementary Material Available: Figures containing UV/vis spectra of F430 and 12,13-diepimeric F430 in H₂O, expansions of a 2D HOHAHA spectrum with the labeled *J*-network associated with the H4 proton at lower contour levels, portions of HMBC spectra, experimental and back-calculated NOE build-up profiles, and superposition of DG21-60(+NOE) structures as well as tables of pairwise RMSD values for DG/SA and X-ray structures (14 pages). Ordering information is given on any current masthead page.

Electron Transfer and Bond Breaking. Examples of Passage from a Sequential to a Concerted Mechanism in the Electrochemical Reductive Cleavage of Arylmethyl Halides

Claude P. Andrieux, Annie Le Gorande, and Jean-Michel Savéant*

Contribution from the Laboratoire d'Electrochimie Moléculaire de l'Université de Paris 7, Unité Associée au CNRS N° 438, 2 place Jussieu, 75251 Paris Cedex 05, France.

Received January 29, 1992. Revised Manuscript Received April 1, 1992

Abstract: A systematic investigation of the kinetics of the electrochemical reduction of a series of 11 arylmethyl halides in acetonitrile and *N,N'*-dimethylformamide reveals a striking change in the reductive cleavage mechanism as a function of the energy of the π^* orbital liable to accept the incoming electron. With ring-substituted nitrobenzyl chlorides and bromides, a stepwise mechanism involving the intermediacy of the anion radical takes place. When slightly less electron-withdrawing substituents, such as nitrile or ester groups, are involved, the reaction occurs via a concerted electron transfer-bond breaking mechanism. This is also observed with the unsubstituted benzyl chloride and bromide as well as with 9-anthracenylmethyl chloride. The main factor then governing the thermodynamics and kinetics of the reductive cleavage is then the dissociation energy of the bond being broken. There is an excellent agreement between the predictions of the recently developed model of dissociative electron transfer and the experimental data both in terms of the quadratic character of the activation-driving force relationship and the magnitude of the intrinsic barrier. In this connection, procedures utilizing the difference in cyclic voltammetric peak potential between two compounds bearing the same nucleofugal group to estimate the difference in their bond dissociation energies are discussed.

Electron transfer to molecules is very often accompanied by the breaking of an existing bond and/or the formation of a new

bond. In the first case, where a radical and an anionic fragment are formed upon electron transfer to a neutral molecule, an im-

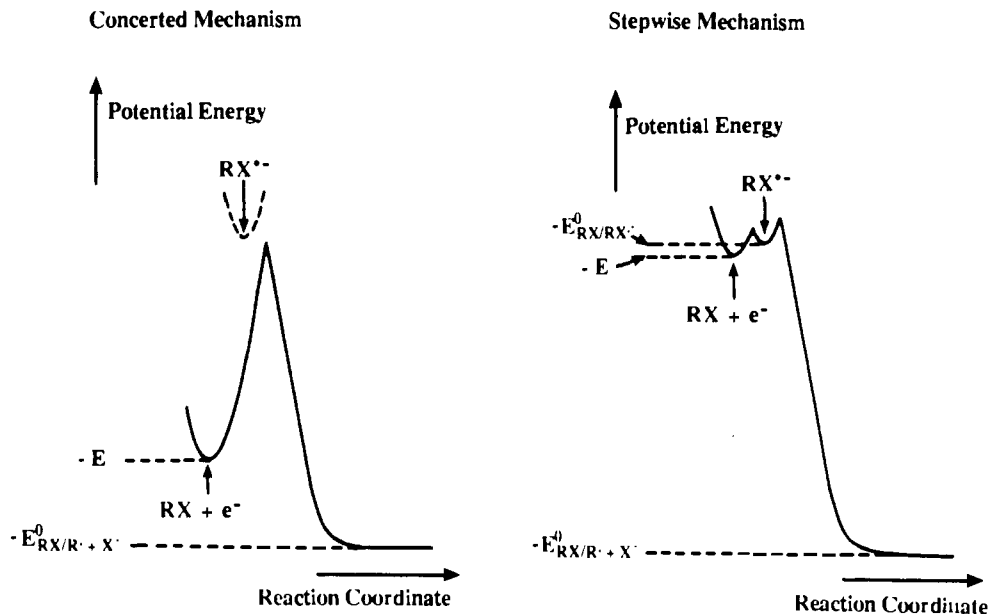


Figure 1. Potential energy diagram showing the passage from a concerted to a stepwise mechanism according to the driving force of the reaction.

portant question is whether electron transfer and bond breaking are concerted or successive steps as sketched in the following scheme:

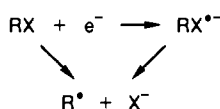


Figure 1 pictures the two situations where, in one case, the anion radical, $\text{RX}^{\bullet-}$, is an intermediate along the reaction pathway, whereas, in the other, the energy of the anion radical is so high that the concerted pathway is energetically more advantageous. This is a central question both in electrochemistry and in conventional homogeneous chemistry. As discussed before, the comprehension of the laws that govern electron transfer bond breaking reactions is important in establishing the strategies that allow one to trigger a radical chemistry or an ionic chemistry upon single electron transfer from outer-sphere homogeneous or heterogeneous electron donors.¹ A typical example of the triggering of radical reactions by outer-sphere electron injection is the $\text{S}_{\text{RN}}1$ substitution reaction at sp^2 and sp^3 carbons bearing a nucleofugal group.² These laws are also useful guidelines for the discussion and prediction of the occurrence of single electron transfer mechanisms in substitution reactions as opposed to the classical $\text{S}_{\text{N}}2$ mechanism.²

The dynamics of the reaction and the structure–reactivity relationships pertaining to the concerted and stepwise mechanisms are expected to be different. When bond breaking and electron transfer are successive, two limiting situations may arise according to which is the rate determining step. If the rate determining step is the bond breaking reaction, the electron transfer step interferes in the overall kinetics solely through its thermodynamic characteristics. If electron transfer is rate determining, the dynamics of the overall reaction is that of an outer-sphere electron transfer. It can thus be described in terms of quadratic activation–driving force relationships such as those derived from the Marcus–Hush model:³

$$\Delta G^{\ddagger} = w_{\text{R}} + \Delta G_0^{\ddagger} \left(1 + \frac{\Delta G^0 - w_{\text{R}} + w_{\text{P}}}{4\Delta G_0^{\ddagger}} \right)^2 \quad (1)$$

(1) (a) See, for example: the introductions of refs 1b and 1c. (b) Andrieux, C. P.; Gallardo, I.; Savéant, J.-M. *J. Am. Chem. Soc.* **1989**, *111*, 1620. (c) Andrieux, C. P.; Grzeszczuk, M.; Savéant, J.-M. *J. Am. Chem. Soc.* **1991**, *113*, 8811.

(2) See, for example: a discussion of this point in ref 4b and references cited therein.

(ΔG^{\ddagger} and ΔG^0 , activation free energy and standard free energy of the forward electron transfer; w_{R} and w_{P} , work required to bring the reactants and products, respectively, from infinite separation to reacting distance). The intrinsic barrier free energy, ΔG_0^{\ddagger} , is the sum of an internal reorganization (bond lengths and angles) factor and a solvent reorganization factor.

In the case of concerted process, i.e., of an electron transfer that possesses an inner-sphere character from the point of view of the acceptor, it has been shown that the above quadratic activation–driving force relationship still applies. However, the intrinsic barrier now contains (besides the reorganization of the bonds not being broken and the reorganization of the solvent) a contribution of the bond breaking process approximately equal to one-fourth of the dissociation energy of the bond being broken.⁴

Most of the previous experimental work concerning concerted and stepwise electron transfer–bond breaking reactions has involved, as model example, the reductive cleavage of carbon–halogen bonds.⁵ With the organic halides thus investigated a sharp distinction has been observed between aromatic and simple aliphatic compounds in the mechanism of their homogeneous or heterogeneous reduction by outer-sphere electron donors in polar solvents.⁶ In the case of aromatic halides the reduction goes through the intermediacy of the anion radicals, whereas with

(3) (a) Marcus, R. A. *J. Chem. Phys.* **1956**, *24*, 4966. (b) Hush, N. S. *J. Chem. Phys.* **1958**, *28*, 962. (c) Marcus, R. A. Theory and Applications of Electron Transfers at Electrodes and in Solution. *Special Topics in Electrochemistry*; Rock, P. A., Ed.; Elsevier: New York, 1977, pp 161–179. (d) Marcus, R. A. *Faraday Discuss. Chem. Soc.* **1982**, *74*, 7.

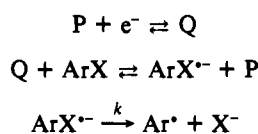
(4) (a) Savéant, J.-M. *J. Am. Chem. Soc.* **1987**, *109*, 6788. (b) Savéant, J.-M. *Adv. Phys. Org. Chem.* **1990**, *26*, 1. (c) The validity of the Morse curve empirical model developed in refs 4a and 4b has recently been confirmed by a series of quantum chemical ab initio calculations on methyl halides.^{4d} (d) Bertran, J.; Gallardo, I.; Moreno, M.; Savéant, J.-M. *J. Am. Chem. Soc.*, in press.

(5) (a) A notable exception is the analysis of the reductive cleavage of carbon–sulfur bonds by heterogeneous or homogeneous (electrogenerated) outer-sphere electron donors.^{5b–f} (b) Griggio, L. *J. Electroanal. Chem.* **1982**, *140*, 155. (c) Griggio, L.; Severin, M. G. *J. Electroanal. Chem.* **1987**, *223*, 185. (d) Arevalo, M. C.; Farnia, G.; Severin, M. G.; Vianello, E. *J. Electroanal. Chem.* **1987**, *220*, 201. (e) Severin, M. G.; Arevalo, M. C.; Farnia, G.; Vianello, E. *J. Phys. Chem.* **1987**, *91*, 466. (f) Severin, M. G.; Farnia, G.; Vianello, E.; Arevalo, M. C. *J. Electroanal. Chem.* **1988**, *251*, 369.

(6) (a) For general reviews on the electrochemistry of organic halides see refs 6b and 6c. For a more recent review and a more detailed discussion on the mechanism of the reduction of aryl halides by outer-sphere homogeneous and heterogeneous electron donors in polar solvents, see ref 4b. (b) Hawley, M. D. In *Encyclopedia of the Electrochemistry of the Elements*; Bard, A. J., Lund, H., Eds.; Wiley: New York, 1980; Vol. XIV, Organic Section. (c) Becker, J. Y. *The Chemistry of Functional Groups, Supplement D*; Patat, S., Rappoport, Z., Eds.; Wiley: New York, 1983; Chapter 6, pp 203–285.

simple aliphatic halides concerted electron transfer–bond breaking prevails.^{4b} These results thus parallel those obtained in the gas phase upon reaction with alkali metals or in apolar or weakly polar matrixes upon γ -rays irradiation at low temperature, lending apparent credit to the notion that the anion radical “exists” in the first case and does not in the second regardless of the reaction medium and the nature of the electron donor reagent.

For the sake of the following discussions, it is useful to recall how the stepwise character of the reductive cleavage in polar solvents of aryl halides and its concerted character in the case of simple aliphatic halides was established.^{4b} With aryl halides, the lifetime of the anion radical, $\text{ArX}^{\cdot-}$, varies considerably (over more than 10 orders of magnitude) according to the nature of Ar and X. Thus, in the 10^{-10} – 10^{-7} -s range of lifetimes, direct electrochemical methods, such as cyclic voltammetry or double potential step chronoamperometry (using ultramicroelectrodes in the 10^{-3} – 10^{-7} -s region) allow one to detect the anion radical and determine its first order decay rate constant. In such cases, there is thus clear evidence of the intermediacy of the anion radical and therefrom of the stepwise character of the reductive cleavage. In the 10^{-6} – 10^{-9} -s range one may use indirect electrochemical methods, such as redox catalysis:



(P/Q being a reversible outer-sphere one-electron redox couple) where the detection of the competition between the reverse electron transfer and the first order decay of $\text{ArX}^{\cdot-}$ provides evidence of the intermediacy of the anion radical and can be used to determine its lifetime. Below 10^{-9} s, the forward electron transfer is rate determining in most cases preventing kinetic access of the decay of $\text{ArX}^{\cdot-}$. However, evidence for the intermediacy of the anion radical may be gained from the experimental observation that the reverse electron transfer is under diffusion control.

Reductive cleavage of simple aliphatic halides by heterogeneous as well as homogeneous outer-sphere electron donor is kinetically controlled by electron transfer in all cases. In direct electrochemistry at inert electrodes (glassy carbon), the transfer coefficient (symmetry factor) is significantly lower than 0.5 (0.2–0.3). Dissociative electron transfer theory⁴ predicts that the activation–driving force relationship has the same quadratic form (eq 1) as in the case of outer-sphere electron transfer and thus that the symmetry factor, α , varies linearly with the driving force:

$$\alpha = 0.5 \left(1 + \frac{\Delta G^0}{4\Delta G_0^*} \right) \quad (2)$$

being smaller than 0.5 for large driving forces. Thus for both mechanisms, rate determining outer-sphere electron transfer leading to the anion radical as an intermediate as well as for the concerted mechanism, the fact that α is much smaller than 0.5 indicates that the standard potential of the relevant reaction, $\text{RX} + \text{e}^- \rightarrow \text{RX}^{\cdot-}$ or $\text{RX} + \text{e}^- \rightarrow \text{R}^{\cdot} + \text{X}^-$, is largely positive to the reduction potential. This is certainly true in the second case, but is it not in the first case as well? There is no direct access to the $\text{RX}/\text{RX}^{\cdot-}$ standard potential in the case of simple aliphatic halides. There is however an indirect way to go around this difficulty. The standard potential of the $\text{RX}/\text{RX}^{\cdot-}$ is certainly negative to that of the corresponding $\text{PhX}/\text{PhX}^{\cdot-}$ couple. The latter is known to be negative to the effective reduction potential of RX . Therefore, a fortiori, the driving force of the $\text{RX} + \text{e}^- \rightarrow \text{RX}^{\cdot-}$ reaction is not in the right direction for an α value lower than 0.5 to be observed. This reasoning thus excludes the occurrence of the outer-sphere mechanism and therefrom establishes that the reaction follows the concerted mechanism.

The reductive cleavage of perfluoroalkyl halides, R_fX , is an interesting borderline case where an anion radical, or at least a loose $\text{R}_f^{\cdot-}$, X^- adduct, is formed in the gas phase or in apolar or weakly polar solid matrixes at low temperature,^{7a-c} whereas re-

duction by outer-sphere electron donors in polar solvents seems to give rise to a concerted electron transfer–bond breaking reaction.^{7f,g}

This example suggests that the mechanism of reductive cleavages may change from stepwise to concerted according to the nature of the reaction medium. As suggested earlier,^{8a} it may also change according to the reducing power of the outer-sphere electron donor reagent, i.e., in other words according to the driving force of the reaction, as can be seen on the schematic potential energy diagram in Figure 1.^{8b,c}

It follows that what governs the nature of the reductive cleavage mechanism is not so much the “existence”, taken in absolute terms, of the anion radical but rather the energetic advantage offered by one mechanism over the other.

Turning back to the sharp difference of behavior between aromatic and simple aliphatic halides, a qualitative explanation of this difference is that the incoming electron can be accommodated transiently in the relatively low energy π^* orbital of the aromatic moiety, whereas no such possibility exists with simple aliphatic halides. In the latter case, at carbon–halogen distances close to that in the ground state, the σ^* orbital energy is so high that concerted electron transfer–bond breaking is energetically more favorable. The fact that the carbon–halogen bond is stronger in aryl halides than in simple aliphatic halides is also an important factor of the difference in the reductive cleavage mechanisms.

In benzyl halides, or more generally, in arylmethyl halides, a π^* orbital is available as in aryl halides but the carbon–halogen bond is significantly weaker. The question of the mechanism of reductive cleavage, stepwise or concerted, thus arises again.

The work reported below was an attempt to answer this question by examining the kinetics of the electrochemical reduction of an extended series of arylmethyl halides at inert electrodes. It will be shown that the reaction mechanism is not the same in the whole family of compounds. It passes from stepwise to concerted according to the nature of the aryl moiety as a function of the energy of the π^* orbital liable to accommodate the incoming electron. For the members of the series the reductive cleavage of which follows the concerted mechanism, the applicability of the dissociative electron transfer theory mentioned above⁴ will be discussed in relation with recent methodologically independent determinations of the carbon–halogen bond dissociation energy in a series of 4-substituted benzyl bromides.⁹ Although we followed an electrochemical approach, the conclusions we reached are expected to extend to homogeneous electron transfer chemistry. Medium and driving force effects that may affect these conclusions when passing from the present to other experimental conditions will be discussed.

Although providing previous pieces of information, earlier studies of the reductive cleavage of the carbon–halogen bond in

(7) (a) Compton, R. N.; Reinhart, P. W.; Cooper, C. C. *J. Chem. Phys.* **1978**, *68*, 4360. (b) Hasegawa, A.; Williams, S. *Chem. Phys. Lett.* **1977**, *46*, 66. (c) Hasegawa, A.; Shiatani, M.; Williams, S. *Faraday Discuss. Chem. Soc.* **1977**, *157*. (d) Kuhn, A.; Illenberger, E. *J. Phys. Chem.* **1989**, *93*, 7060. (e) Kuhn, A.; Illenberger, E. *J. Chem. Phys.* **1990**, *93*, 357. (f) Andrieux, C. P.; Gélis, L.; Médebelle, M.; Pinson, J.; Savéant, J.-M. *J. Am. Chem. Soc.* **1990**, *112*, 3509. (g) The demonstration that the reaction follows a concerted mechanism is less straightforward than in the case of simple aliphatic halides because a reasonable maximization of the standard potential of the $\text{R}_f\text{X}/\text{R}_f\text{X}^{\cdot-}$ couple is not as easy to achieve. However the standard potential and intrinsic barrier derived from the electrochemical experiments are clearly more consistent with the concerted mechanism than with the stepwise mechanism. Recent ab initio quantum chemical calculations on CF_3Cl , incorporating a modelization of the effects of polar solvent, have confirmed and explained the change in mechanism that occurs under the influence of a polar solvent.^{4d}

(8) (a) Andrieux, C. P.; Merz, A.; Savéant, J.-M. *J. Am. Chem. Soc.* **1985**, *107*, 6097. (b) For simplicity, the potential energy diagrams are represented in Figure 1 as functions of a single reaction coordinate, the carbon–halogen distance. This is certainly the main reaction coordinate for the three reactions, but solvent reorganization is also likely to play a role. Rigorously speaking it should therefore be included in the set of reaction coordinates although this does not change the general picture sketched in Figure 1 of the passage from stepwise to concerted mechanism as a function of the driving force. (c) Some experimental evidence of such a passage has been found in the homogeneous reduction of triphenylmethylphenyl sulfides by electrochemically generated aromatic anion radicals.^{5f}

(9) Clark, K. B.; Wayner, D. D. M. *J. Am. Chem. Soc.* **1991**, *113*, 9363.

benzyl-type halides do not provide unequivocal answers to the questions raised above. Phenyl-substituted nitrobenzyl halides have attracted particular attention because 4-nitrobenzyl halides have been the first examples of substrates undergoing $S_{RN}1$ substitution reactions at a sp^3 carbon.¹⁰ Cyclic voltammograms of 2-, 3-, and 4-nitrobenzyl chlorides and bromides at a platinum electrode in acetonitrile have been interpreted as resulting from the initial formation of the corresponding anion radical followed by the expulsion of the halides ion and dimerization of the ensuing nitrobenzyl radical.¹¹ Direct evidence of the intermediacy of the anion radical in the electrochemical reduction was actually obtained only in the case of 3-nitrobenzyl chloride from the variation of the apparent number of electrons with time in potential step chronoamperometry.^{11a} The assumption that the same is true for the 2- and 4-derivatives gets some support from the direct observation of the anion radicals (by means of their UV-vis spectra) in pulse radiolysis in water at room temperature.^{12a-d} The formation of the anion radicals from 2-, 3-, and 4-nitrobenzyl bromides and 3- and 4-nitrobenzyl iodides was also observed under the same experimental conditions.^{12a,b} The anion radicals of 4-nitrobenzyl chloride and bromide have also been detected by ESR spectroscopy upon γ -rays irradiation of the parent compound in a solid matrix at 77 K.¹³ As discussed earlier these observations do not necessarily prove the intermediacy of the anion radical under the conditions of the electrochemical reduction (which are milder in terms of driving force) and in different media.^{14a}

Comparison of the pulse radiolysis behavior of cyanobenzyl halides with that of the corresponding nitro derivatives in water shows that the anion radicals are cleaved much more rapidly in the first case than in the second.^{14a} The cleavage rate constant could be determined only with the *m*-cyano compound and found to be five orders of magnitude larger than with the correspondent nitro derivative.

There are rather few electrochemical studies of other benzyl-type halides on inert electrodes.^{14b} The reduction of benzyl chloride, bromide, and iodide themselves at platinum or glassy carbon electrodes in acetonitrile has been considered to probably occur via a dissociative electron transfer reaction¹⁵ by analogy with simple aliphatic halides in the absence of solid experimental evidence. Electron attachment to the same benzyl halides has also been investigated using UV or γ -rays irradiation at 77 K in solid matrices.¹⁶ Benzyl radical-halide adducts were observed by means of their UV-vis spectra, and their characteristics shown to depend upon the nature of the halogen and the polarity of the matrix. The electrochemical reduction of two compounds of the triphenylmethyl chloride family (9-chloro-9[α -(9-fluorenylidene)benzyl]fluorene and 9-chloro-9-mesitylfluorene)

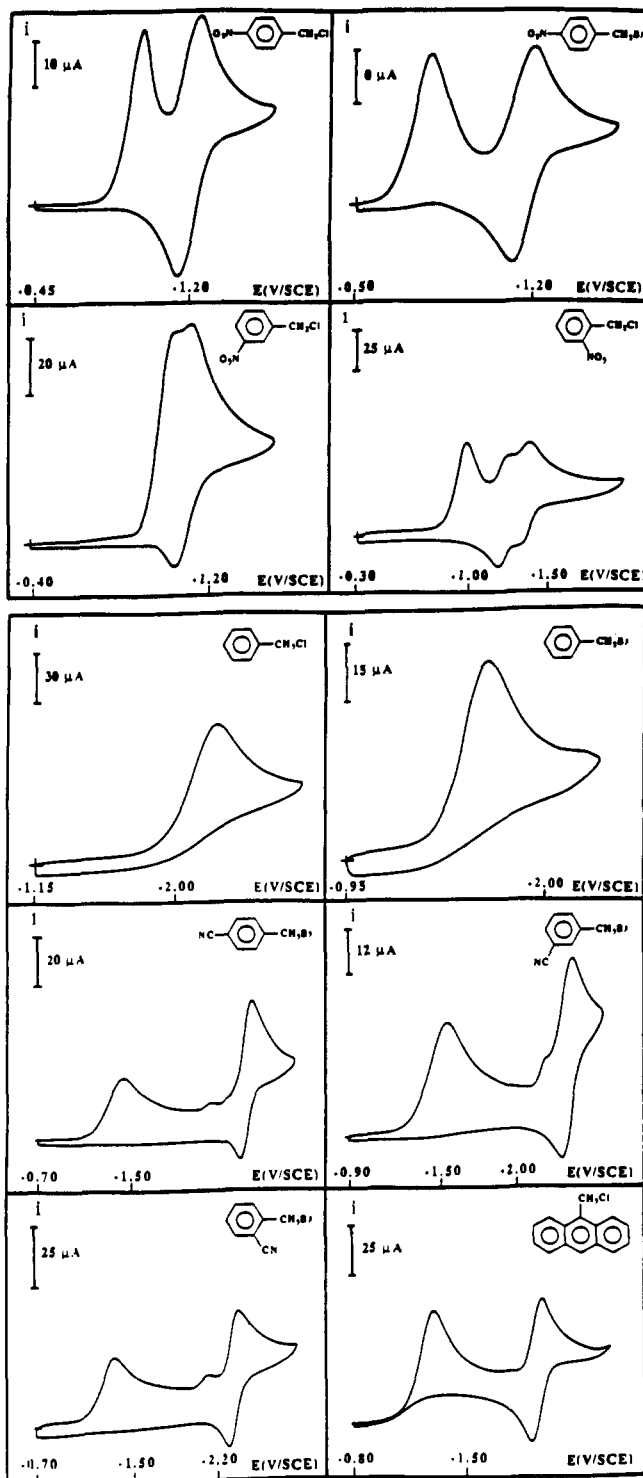


Figure 2. Cyclic voltammetry of arylmethyl halides (2 mM) in DMF + 0.1 M $n\text{-Bu}_4\text{NBF}_4$ at a glassy carbon electrode: scan rate, $0.1 \text{ V}\cdot\text{s}^{-1}$; temperature, 25°C .

at a platinum electrode in acetonitrile has been shown to occur according to the concerted mechanism on the basis of low value of the symmetry factor (transfer coefficient) and a high value of the intrinsic barrier.^{8a} In a closely related family of compounds, ring-substituted 9-chlorofluorenes, it has been shown that a good linear correlation exists between the reduction potential of the chlorides and the oxidation potential of the conjugate bases of the corresponding fluorenes, with however no investigation of the concerted or the stepwise character of the reductive cleavage.¹⁷

(10) (a) Kornblum, N.; Michel, R. E.; Kerber, R. C. *J. Am. Chem. Soc.* **1966**, *88*, 5662. (b) Russel, G. A.; Danen, N. C. *J. Am. Chem. Soc.* **1966**, *88*, 5663.

(11) (a) Lawless, J. G.; Bartak, D. E.; Hawley, M. D. *J. Am. Chem. Soc.* **1969**, *91*, 7121. (b) Peterson, P.; Carpenter, A. K.; Nelson, R. F. *J. Electroanal. Chem.* **1970**, *27*, 1. (c) Bartak, D. E.; Hawley, M. D. *J. Am. Chem. Soc.* **1972**, *94*, 640.

(12) (a) Neta, P.; Behar, D. *J. Am. Chem. Soc.* **1980**, *102*, 4798. (b) Bays, J. P.; Blumer, S. T.; Baral-Tosh, S.; Behar, D.; Neta, P. *J. Am. Chem. Soc.* **1983**, *105*, 320. (c) Norris, R. K.; Barker, S. D.; Neta, P. *J. Am. Chem. Soc.* **1984**, *106*, 3140. (d) Meot-Ner, M.; Neta, P.; Norris, R. K.; Wilson, K. J. *Phys. Chem.* **1986**, *90*, 168.

(13) Symons, M. C. R.; Bowman, W. R. *J. Chem. Soc., Chem. Commun.* **1984**, 1445.

(14) (a) As noted earlier,^{11c} cleavages of anion radicals containing a nucleofugal group seem to be distinctly slower in water than in organic aprotic solvents. (b) In contrast with abundant early polarographic studies (for a review see ref 6b). In these cases, the electrode material, mercury, most probably interferes in the course of the reduction mechanism in most cases. The results thus obtained are therefore not very useful to the present discussion of the mechanism of electron transfer (and bond breaking) from outer-sphere electron donors.

(15) Koch, D. A.; Henne, B. J.; Bartak, D. E. *J. Electrochem. Soc.* **1987**, *134*, 3062.

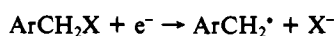
(16) (a) Irie, M.; Shimizu, M.; Yoshida, H. *J. Phys. Chem.* **1976**, *80*, 2008. (b) Izumida, T.; Ichikawa, T.; Yoshida, H. *J. Phys. Chem.* **1979**, *83*, 373. (c) Izumida, T.; Fujii, K.; Ogasawara, M.; Yoshida, H. *Bull. Soc. Chim. Jpn.* **1983**, *56*, 82.

(17) Maran, F.; Vianello, E. *Tetrahedron Lett.* **1990**, *31*, 5803.

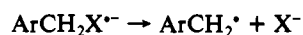
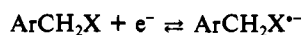
Results

Most of the cyclic voltammetric experiments described below were carried out at glassy carbon electrodes. In the cases where very high scan rates were used in an attempt to overrun the instability of anion radical, the working electrode was a gold ultramicroelectrode (diameter: 5 or 17 μm).^{18a} It was checked that, at lower scan rates with usual microelectrodes (diameters in the millimeter range), glassy carbon and gold give rise to the same cyclic voltammetric behavior. All compounds were studied in *N,N'*-dimethylformamide (DMF) as a solvent. In some cases, comparison was made with acetonitrile.

Figure 2 gives an overview of the low scan rate cyclic voltammetry of all compounds investigated in DMF. With the exception of benzyl chloride and bromide themselves, which show a single irreversible broad wave in the available potential window, all compounds (ArCH_2X) exhibit two main waves. The first is irreversible, at least at low scan rates. The second is reversible and corresponds to the reversible reduction of either the monomeric hydrocarbon, ArCH_3 , or the dimer $\text{ArCH}_2\text{CH}_2\text{Ar}$ (in the case of 2-nitrobenzyl chloride, the second wave is split into two closely spaced reversible waves that correspond, as noted earlier,^{11a} to the stepwise reduction of the ortho-ortho' dimer). The first waves thus correspond to the reductive cleavage of the starting halide into the arylmethyl radical and the halide ion. This may occur concertedly



or stepwisely

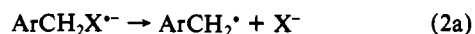


As already appears in Figure 2, from the shape of the first wave and potential distances between first and second waves, and will become even more evident in the following, the compounds investigated fall into two categories: the nitro derivatives and the other compounds.

Nitrobenzyl Halides

3-Nitrobenzyl chloride is the simplest compound in the series to study. The variations of its cyclic voltammograms with the scan rate on a conventional gold microelectrode are shown in Figure 3 (the same results were obtained at a glassy carbon electrode). Upon raising the scan rate, one passes from a set of two closely spaced one-electron waves, with the first irreversible and the second reversible, to a single one-electron reversible wave. The peak potential of the first wave varies first linearly with the log of the scan rate and then levels off reaching a constant value.

These observations show unambiguously that the anion radical is formed as an intermediate. The value of the $E_p - \log v$ slope at low scan rate, -28 mV, and that of the peak width, $E_{p/2} - E_p = 50$ mV (E_p , peak potential; $E_{p/2}$, half-peak potential) indicate^{18b} that the rate determining step is a first order reaction following the uptake of one electron

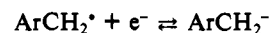


The one-electron per molecule stoichiometry is compatible with a follow-up dimerization of the 3-nitrobenzyl radical



although further reduction at the electrode and/or in the solution

(18) (a) Andrieux, C. P.; Hapiot, P.; Savéant, J.-M. *Chem. Rev.* **1990**, *90*, 723. (b) Andrieux, C. P.; Savéant, J.-M. In *Electrochemical Reactions in Investigation of Rates and Mechanisms of Reactions, Techniques of Chemistry*; Bernasconi, C. F., Ed.; Wiley: New York, 1986; Vol. VI/4E, Part 2, pp 305–390. (c) Andrieux, C. P.; Hapiot, P.; Savéant, J.-M. *J. Phys. Chem.* **1988**, *92*, 5987. (d) Nadjo, L.; Savéant, J.-M. *J. Electroanal. Chem.* **1973**, *48*, 113.



and/or



followed by



cannot be excluded since the 3-nitrobenzyl radical has a reduction potential well positive (of the order of -0.65 V vs SCE¹⁹) of that of the 3-nitrobenzyl chloride itself.

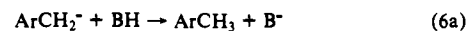
The rate constant of the cleavage of the radical anion is readily derived from the intersection of the oblique and horizontal linear portions of the $E_p - \log v$ plots^{18b} and found equal to 80 s⁻¹, i.e., somewhat larger than previously found in acetonitrile (2.5 s⁻¹^{11a}). The standard potential of the 3-nitrobenzyl chloride/3-nitrobenzyl chloride anion radical is thus found to be -1.04 V vs SCE only slightly positive to those of 3-nitrotoluene (-1.10) and nitrobenzene (-1.08).

4-Nitrobenzyl Chloride. In this case also the cyclic voltammetric curves at low and moderate scan rates are the same at gold and glassy carbon electrodes. The first wave is a one-electron irreversible wave the peak potential of which varies linearly with the log of the scan rate (Figure 4) by -38 to -40 mV per unit with a peak width, $E_{p/2} - E_p = 60$ mV. The second one-electron reversible wave does not change in shape and location with the scan rate. This overall behavior, particularly the irreversibility of the first wave, remains the same in the whole range of scan rates that are accessible with conventional microelectrodes (disks having a diameter in the millimeter range), i.e., up to a few thousands volts per second. The use of a gold ultramicroelectrode allowed the observation of the chemical reversibility of the first wave (see Figure 4) thus demonstrating the intermediacy of the anion radical in the reductive cleavage reaction. The reductive cleavage mechanism is thus the same as in the preceding case,²⁰ but the cleavage of the anion radical is much faster. From the cyclic voltammograms obtained at high scan rates it was derived, taking the iR drop and double layer charging effects into account^{18a,c} that the anion radical cleavage rate constant is $k = 4.0 \times 10^6$ s⁻¹,²¹ the standard potential of the 4-nitrobenzyl chloride-/4-nitrobenzyl chloride anion radical couple is -1.14 V vs SCE, and the apparent (not corrected from double layer effects) standard rate constant characterizing this redox couple is $k_{sp}^{\text{app}} = 1$ cm²s⁻¹.

The characteristics of the irreversible wave observed at low and moderate scan rates are consistent with the rate constant values thus determined as results from the following reasons. The irreversible wave corresponds to an "EC" (E, electron transfer (1a); C, first order cleavage of the anion radical (2a)) mechanism. There is a competition between the "E" and the "C" steps for the kinetic control of the wave. When the transfer coefficient is close to 0.5, as likely to be the case in the present conditions, the kinetic competition is governed by the ratio^{18b,d}

(19) (a) The standard reduction potential of the 3-nitrobenzyl radical itself has not been determined. However it can be estimated from a Hammett correlation using data pertaining to other ring-substituted benzyl radicals.^{19b} (b) Sim, B. A.; Milne, P. H.; Griller, D.; Wayner, D. D. M. *J. Am. Chem. Soc.* **1990**, *112*, 6635.

(20) I.e., the electron uptake and the cleavage of the anion radical may be followed by reactions 3a–5a and, in addition, by



(BH being the strongest proton donor present in the reaction medium.) Reaction 6a seems to be a more likely source of ArCH_3 than H-atom abstraction from the solvent by ArCH_2^\bullet radicals,^{11a} since the latter are not particularly good H-atom scavengers, whereas reactions 3a and 4a are certainly rapid in view of their large driving forces. Preparative scale electrolysis at -0.90 V vs SCE at a carbon electrode of a 10 mM solution consumed 1.3 electrons per molecule and resulted in the formation of 53% of the $\text{ArCH}_2\text{—CH}_2\text{Ar}$ dimer and 28% of 4-nitrotoluene.

(21) This was significantly larger than a previous estimate in acetonitrile.^{11a} The latter was however based on an indirect estimation of the standard potential of the 4-nitrobenzyl chloride/4-nitrobenzyl chloride anion radical.

$$\frac{(k_S^{ap})^2}{Dk^{1/2}} \left(\frac{RT}{Fv} \right)^{1/2}$$

With the values obtained for k and k_S^{ap} and taking $D = 10^{-5} \text{ cm}^2\text{-s}^{-1}$, it is predicted that the competition ratio varies from 2.5 to 25 between 0.1 and $10 \text{ V}\cdot\text{s}^{-1}$ and thus that $\partial E_p/\partial \log v$ should be equal to 40 mV and $E_{p/2} - E_p$ should fall in the range 52–58 mV, in good agreement with the experimental data.

Even if it would have proven impossible to reach scan rates high enough for overbalancing the decomposition of the anion radical, values of $-\partial E_p/\partial \log v$ and $E_{p/2} - E_p$ of the order of 40 and 60 mV (at 25°C) would have been by themselves, clear enough indications of the intermediacy of the anion radical in the reductive cleavage process. Indeed, if a concerted mechanism would have occurred, the above values would have corresponded to a value of α of the order of 0.8 indicating, as discussed in the introduction, that the reduction potential would have been much positive to the standard potential of the rate determining step, i.e., $\text{ArCH}_2\text{X} + e^- \rightarrow \text{ArCH}_2^* + \text{X}^-$, which obviously does not make any sense.

The standard potential of the 4-nitrobenzyl chloride/4-nitrobenzyl chloride anion radical (-1.14 V vs SCE) is only slightly positive to that of 4-nitrotoluene (-1.18) and slightly negative to that of nitrobenzene (-1.08). At the same low scan rate, the two reduction waves are closer one to the other in the 3- derivative than in the 4-derivative. This is essentially a reflection of the fact that the cleavage is slower in the first case than in second.

4-Nitrobenzyl Bromide. A detailed study of this compound is more difficult than that of the chloride owing to adsorption and irreproducibility on gold and platinum electrodes. Conclusions can however be drawn from the cyclic voltammetry of this compound at a glassy carbon electrode between 0.1 and $10 \text{ V}\cdot\text{s}^{-1}$. In this range, the cyclic voltammetry shows two successive one-electron waves, the first being irreversible and the second reversible (Figure 2). The peak potential of the first wave varies linearly with the logarithm of the scan rate by -45 mV in average with $E_{p/2} - E_p = 65 \text{ mV}$ in average. As discussed earlier, these values are typical of an EC reaction scheme with a mixed kinetic control by the E and C steps. It may thus be concluded that the same mechanism as in the preceding case, involving the intermediacy of the anion radical, takes also place here. The cleavage of the anion radical is certainly much faster than in the case of the chloride since, at the same scan rate, the distance between the two waves increases substantially (from 0.26 to 0.40 V at $0.1 \text{ V}\cdot\text{s}^{-1}$) upon passing from the chloride to the bromide (Figure 2). The cleavage is now too fast for its rate constant to be determined precisely through any direct electrochemical technique even with the help of ultramicroelectrodes.

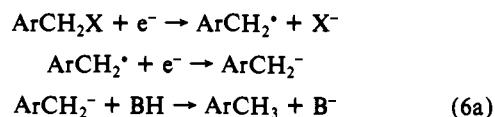
2-Nitrobenzyl Chloride. As noted earlier, the most striking difference with the other nitrobenzyl halides is the fact that there are now two closely spaced reversible second waves instead of one (Figure 2). As shown previously,^{11a} this wave splitting characterizes the cyclic voltammetric behavior of the 2,2'-dinitrodibenzyl dimer as opposed to the other isomers. The reductive cleavage that occurs at the first one-electron irreversible wave follows the same stepwise mechanism as in the preceding cases as attested by the average values of $-\partial E_p/\partial \log v$ (45 mV) and of $E_{p/2} - E_p$ (70 mV) found at a glassy carbon electrode between 0.05 and $10 \text{ V}\cdot\text{s}^{-1}$. There is again mixed kinetic control of the reduction by the electron transfer step and the cleavage of the anion radical.

All the other arylmethyl compounds have in common cyclic voltammetric features that were not found with the nitro derivatives. The best way to make reliable comparisons between the various compounds in the series is to examine their cyclic voltammetric behavior at glassy carbon electrode at low and moderate scan rates ($0.1\text{--}10 \text{ V}\cdot\text{s}^{-1}$). The use of gold or platinum electrodes is precluded for all compounds but 9-anthracenylmethyl chloride by the appearance of adsorption-shaped peaks and trace crossings upon scan reversal at the level of the first wave (as already observed in the cyclic voltammetry of benzyl bromide in acetonitrile at a platinum electrode¹³). Under the conditions defined above the first wave is, in all cases, irreversible and broad, much broader than with the nitro derivatives. Its peak potential varies linearly

with the logarithm of the scan rate, as with the nitro derivatives but with slopes that are much larger (100 mV on the average instead of $30\text{--}50 \text{ mV}$). At the same time, the distance between the peaks of the two successive waves (when there is a second wave, i.e., in all cases but PhCH_2Cl and PhCH_2Br) is much larger than with the nitro derivatives (at least 700 mV at $0.1 \text{ V}\cdot\text{s}^{-1}$ instead of 400 mV at most at the same scan rate).

The broadness of the first waves and the large slopes of the $E_p - \log v$ plots indicate that the reduction is governed by the kinetics of an electron transfer step and not, even partly, by that of a follow-up chemical step. In addition to this, the transfer coefficient (symmetry factor) of the rate-controlling electron transfer step is distinctly lower than 0.5 (ca. 0.3) indicating a situation in which the reduction potential is clearly negative to the standard potential characterizing the electron transfer rate determining step. We have thus a first indication that the reductive cleavage follows a concerted mechanism.

More precise results concerning the transfer coefficient were obtained taking advantage of the following observations. With benzyl chloride, benzyl bromide, and 9-anthracenylmethyl chloride, the electron stoichiometry of the irreversible wave is 2 both in acetonitrile and DMF whatever the scan rate.²² This falls in line with the formation of the arylmethyl radical at, or close to, the electrode surface followed by rapid reduction since the standard potential of the $\text{ArCH}_2^*/\text{ArCH}_2^-$ couple is in all three cases positive to the reduction potential of the halides.¹⁹



(BH: strongest proton donor present). This rapid reduction of the arylmethyl radicals would prevent their dimerization in contrast to what was happening with the nitro derivatives.

With the ring substituted cyanobenzyl bromides, the electron stoichiometry varies with the scan rate, tending toward 2 as the scan rate increases. A likely interpretation of these observations, falling in line with previous findings on the role of electrogenerated bases, in the framework of the above reaction scheme, is that ArCH_2^- and/or B^- reacts with the starting material along a substitution reaction yielding the bibenzyl dimer and/or ArCH_2B .



These reactions are not very rapid since the suppression of their effect does not require large scan rates (of the order of a few $\text{V}\cdot\text{s}^{-1}$ at most). The fact that they interfere in the case of the ring-substituted cyanobenzyl bromides, and not with benzyl bromide itself, is to be related to the enhancement of the electrophilic character of the benzylic carbon ensuing from the ring substitution by the electron-withdrawing cyanide group.

Addition of an acid such that its conjugate base would be too weak to react with the cyanobenzyl bromide substrate should suppress the observed effect and lead to an electron stoichiometry of 2, independent of the scan rate. This is indeed what was observed upon addition of phenol or benzoic acid in amounts not exceeding 50 mM . At the same time, we have noted that the addition of these acids also suppress the small waves that are observed at the foot of the main second one-electron reversible waves in all three cases (Figure 2). Since this point was not central to the main purpose of our study, we did not pursue for the

(22) This was determined by comparison with the first one-electron reversible wave of anthracene in the same medium, taking into account that^{18b} for the reversible wave of anthracene, the peak current density:

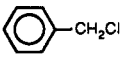
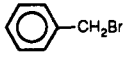
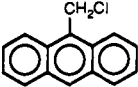
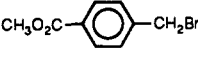
$$i_p = 0.446FC^0D^{1/2}(Fv/RT)^{1/2}$$

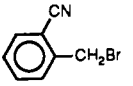
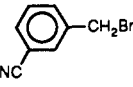
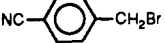
(C^0 , bulk concentration of the substrate; D , its diffusion coefficient; v , scan rate), whereas for the irreversible wave

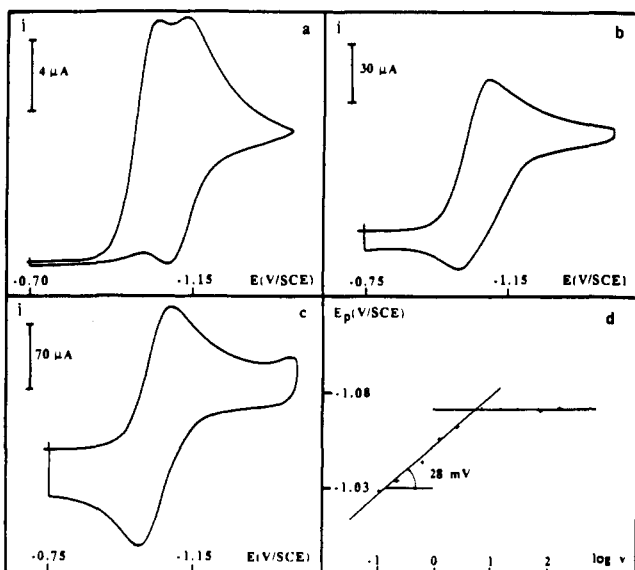
$$i_p = 0.496FC^0D^{1/2}(\alpha Fv/RT)^{1/2}$$

where α , the transfer coefficient, is derived from the peak width according to eq 4.

Table I. Peak Potentials and Determination of the Transfer Coefficient, α , from the Cyclic Voltammetric Peak Widths and from the $E_p - \log v$ Plots^a

compound	scan rate (V·s ⁻¹)	medium									
		DMF				CH ₃ CN					
		$-E_p$ (V vs SCE)	$E_{p/2} - E_p$ (mV)	α	$-\frac{\partial E_p}{\partial \log v}$ (mV)	α	$-E_p$ (V vs SCE)	$E_{p/2} - E_p$ (mV)	α	$-\frac{\partial E_p}{\partial \log v}$ (mV)	α
	0.1	2.21	155	0.30 ₈			2.24	155	0.30 ₈		
	1.0	2.30	150	0.31 ₈			2.34	160	0.29 ₈		
	10	2.41	170	0.28 ₁			2.44	160	0.29 ₈		
	av		158	0.30 ₂	97	0.30 ₅		158	0.30 ₂	104	0.28 ₈
	0.1	1.71	140	0.34 ₁			1.74	140	0.34 ₁		
	1.0	1.82	145	0.32 ₉			1.84	140	0.34 ₁		
	10	1.94	150	0.31 ₈			1.96	160	0.29 ₈		
	av		145	0.32 ₉	98	0.30 ₆		147	0.32 ₄	98	0.30 ₆
	0.1	1.29	120	0.39 ₈			1.41	115	0.41 ₅		
	1.0	1.36	125	0.38 ₂			1.49	115	0.41 ₅		
	10	1.44	130	0.36 ₇			1.57	120	0.39 ₈		
	av		125	0.38 ₂	82	0.36 ₁		117	0.40 ₈	76	0.39 ₅
	0.1										
	1.0										
	10	1.56	140	0.34 ₁			1.64	130	0.36 ₀		
	av										

compound	scan rate (V·s ⁻¹)	medium									
		DMF + 50 mM benzoic acid				DMF + 50 mM phenol					
		$-E_p$ (V vs SCE)	$E_{p/2} - E_p$ (mV)	α	$-\frac{\partial E_p}{\partial \log v}$ (mV)	α	$-E_p$ (V vs SCE)	$E_{p/2} - E_p$ (mV)	α	$-\frac{\partial E_p}{\partial \log v}$ (mV)	α
	0.1	1.44	130	0.36 ₇			1.44	140	0.34 ₁		
	1.0	1.53	150	0.31 ₈			1.54	145	0.32 ₉		
	10	1.63	165	0.28 ₉			1.64	155	0.30 ₈		
	av		148	0.32 ₃	98	0.30 ₆		147	0.32 ₅	102	0.29 ₀
	0.1	1.62	140	0.34 ₁			1.66	150	0.31 ₈		
	1.0	1.72	150	0.31 ₈			1.76	150	0.31 ₈		
	10	1.83	180	0.26 ₅			1.87	175	0.27 ₃		
	av		157	0.30 ₄	105	0.28 ₂		158	0.30 ₁	108	0.27 ₈
	0.1	1.46	140	0.34 ₁			1.48	140	0.34 ₁		
	1.0	1.54	145	0.32 ₉			1.58	140	0.34 ₁		
	10	1.65	160	0.29 ₈			1.68	160	0.29 ₈		
	av		148	0.32 ₃	88	0.34 ₁		147	0.32 ₄	100	0.29 ₆

^aIn DMF or CH₃CN + 0.1 M *n*-Bu₄NBF₄, at a glassy carbon electrode at 25 °C.**Figure 3.** Cyclic voltammetry of 3-nitrobenzyl chloride (2 mM) in DMF + 0.1 M *n*-Bu₄NBF₄ at a gold disk electrode as a function of the scan rate: (a) 0.2, (b) 20, and (c) 100 V·s⁻¹. (d) Variations of the peak potential of the first wave with the scan rate. Temperature, 25 °C.

moment investigations aiming at the assignment of these small waves. In the absence of acids, not only does the electron stoichiometry vary with the scan rate but also other characteristics of the wave such as the peak width $E_{p/2} - E_p$ and $\partial E_p / \partial \log v$, i.e., the rate at which the peak potential varies with the scan rate. The values of these experimental quantities from which the transfer coefficient is derived were found not only to be independent of the scan rate in the presence of the aforementioned acids but also to be the same as those found at the upper edge of the range of scan rates in the absence of acid. These values, and the ensuing values of the transfer coefficient, may thus be reliably considered as characterizing the cleavage reaction itself without any interference of the effect of possible follow-up reactions.

Figure 5 shows typical examples of $E_p - \log v$ plots obtained at a glassy carbon electrode. The values of the slopes of these $E_p - \log v$ plots and those of the peak widths are gathered in Table I.²³ The values of the transfer coefficient, α , were derived from the $E_p - \log v$ slopes according to^{18b,d}

$$\alpha = -\frac{F}{2RT} \frac{\partial E_p}{\partial \ln v} \quad (3)$$

and from the peak widths using the following equation:

$$\alpha = \frac{RT}{F} \frac{1.85}{E_{p/2} - E_p} \quad (4)$$

(23) Although the effect of acids was not tested in the case of 4-carbomethoxybenzyl bromide, the values of α obtained from the $E_p - \log v$ plot and the peak width at the upper edge of the scan rate range where the electron stoichiometry is 2 are reported in Table I.

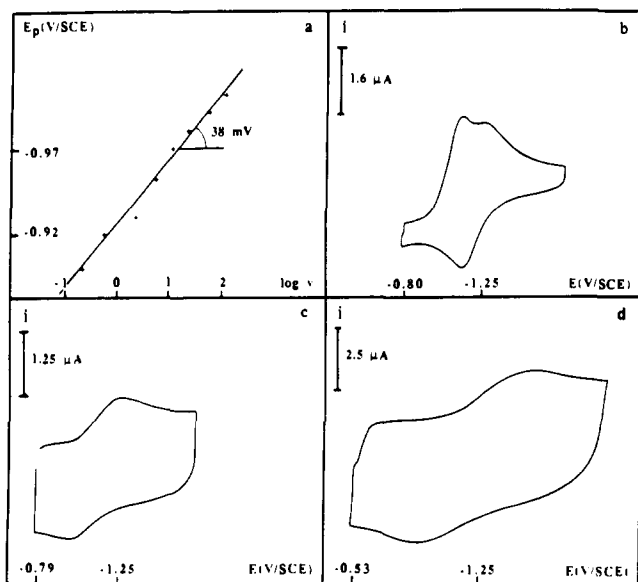


Figure 4. Cyclic voltammetry of 4-nitrobenzyl chloride in DMF + *n*-Bu₄NBF₄ at a gold disc electrode as a function of the scan rate. (a) Variations of the peak potential with the scan rate in the range 0.1–10 V·s⁻¹. Cyclic voltammograms at (a) 1900, (b) 98 000 and (c) 300 000 V·s⁻¹. Electrode diameter: (a) 1 mm, (b) 17 μm, (c and d) 5 μm. 4-Nitrobenzyl chloride concentration (mM): (a) 2 and (b, c, and d) 20. Supporting electrolyte concentration (M): (a) 0.1 and (b, c, and d) 0.4. Temperature: 25 °C.

It is seen that there is a good agreement between the values of the transfer coefficient obtained from either the $E_p - \log v$ slope or the peak width. It is also seen that the results obtained in acetonitrile and DMF are very similar.

Discussion

Stepwise Vs. Concerted Mechanisms. As discussed above, the cyclic voltammetric data provide unambiguous evidence that the electrochemical reductive cleavage of the nitrobenzyl halides investigated follows the stepwise mechanism, i.e., involves the intermediacy of the anion radical.

With all the other compounds the reductive cleavage is under the kinetic control of an heterogeneous electron transfer reaction and its transfer coefficient is distinctly lower than 0.5. This latter observation indicates that the effective reduction potential is, in all these cases, much negative to the standard potential of the redox couple involved in the rate determining step. This condition is certainly obeyed by the $\text{ArCH}_2\text{X}/\text{ArCH}_2^* + \text{X}^-$ couple (as seen in the following from thermochemical estimations, this standard potential falls in the range $-0.75/-0.90$ V vs SCE for PhCH_2Cl and $-0.60/-0.80$ V vs SCE for PhCH_2Br and would have even more positive values for the other chlorides and bromides). However would not this condition be obeyed by the $\text{ArCH}_2\text{X}/\text{ArCH}_2\text{X}^-$ couple as well?

We have noted, during the study of the nitrobenzyl halides, that the standard potential of the $\text{ArCH}_2\text{X}/\text{ArCH}_2\text{X}^-$ couple is not very different from that of the $\text{ArCH}_3/\text{ArCH}_3^{\cdot-}$ couple (100 mV more positive at most). Thus we can obtain a reasonable estimation of the $\text{ArCH}_2\text{X}/\text{ArCH}_2\text{X}^-$ standard potentials in the case where a second reversible wave is observed (cyanobenzyl bromides, 4-carbomethoxybenzyl bromide, and 9-anthracenylmethyl chloride) by adding 100 mV to the mid peak potential of the second reversible wave (Figure 2). We thus see that the reductive cleavage peak potential at 0.1 V·s⁻¹ is 0.6–0.9 V positive to the $\text{ArCH}_2\text{X}/\text{ArCH}_2\text{X}^-$ standard potential according to the compound in this series. With benzyl chloride and bromide no second wave appears as expected from the fact that toluene or even benzene are not reduced before the discharge of the supporting electrolyte cation. These very facts indicate that the $\text{ArCH}_2\text{X}/\text{ArCH}_2\text{X}^-$ standard potential is at least 0.6 V negative to the reaction potential at 0.1 V·s⁻¹ in the case of benzyl chloride and 0.9 V in the case of benzyl bromide. Thus, in all seven cases,

the standard potential of the $\text{ArCH}_2\text{X}/\text{ArCH}_2\text{X}^-$ couple not only is not positive but also is in fact much negative to the reduction potential.

We may therefore conclude that the reductive cleavage in all these seven compounds occurs according to the concerted mechanism. The above reasonings, based on the values of the transfer coefficient, may seem risky for two reasons. One is that the low α values experimentally observed might result from some interfacial phenomena resulting in partial inhibition of the reaction. The other is that the reasonings are based on the quadratic character of the activation-driving force relationship in both the outer-sphere case and dissociative case and that this feature is the result of a rather crude model in both cases.^{3,4} The present series of compounds offer an opportunity to check the validity of the mechanistic conclusions on an entirely different basis involving the values of the reduction potentials rather than those of the transfer coefficient.

Let us thus assume for a moment that the reductive cleavage involves the intermediacy of the anion radical. As the decomposition of the anion radical becomes more and more rapid, the peak potential should shift toward more and more positive values. This positive shift would however stop when the decomposition of the anion radical has become faster than the reverse electron transfer from which it was generated. When this situation is reached the initial electron transfer in the forward direction has become the rate determining step. The peak potential has then reached its most positive value which is related to the kinetics of the forward electron transfer step according to the following equation:^{18b,d}

$$E_p = E^0 - 0.78 \frac{RT}{\alpha F} + \frac{RT}{\alpha F} \ln \frac{k_S^{\text{RP}}}{(D\alpha Fv/RT)^{1/2}}$$

with the same notations as above.

In the study of 4-nitrobenzyl chloride we have found $k_S^{\text{RP}} = 1 \text{ cm}^2\text{s}^{-1}$. This is a reasonable estimate of what could be k_S^{RP} in the whole series. Taking $D = 10^{-5} \text{ cm}^2\text{s}^{-1}$ and $\alpha = 0.5$,²⁴ we find that E_p should be 240 mV positive to the standard potential of the $\text{ArCH}_2\text{X}/\text{ArCH}_2\text{X}^-$ couple at 0.1 V·s⁻¹. Taking into account the earlier estimations of the standard potential we see that these positive shifts are not sufficient, by a large amount, to bring the predicted peak potentials in the vicinity of the experimentally observed peak potentials.

There is thus, for all seven compounds, a perfect consistency of the reasonings based on values of the transfer coefficient with those based on values of the reduction potential therefore leading unambiguously to the conclusion that they all undergo a concerted electron transfer–bond breaking reductive cleavage reaction.

Test of the Theory of Dissociative Electron Transfer. At this point, it is interesting to examine whether the recently developed theory of dissociative electron transfer⁴ can be applied quantitatively to this set of compounds, with regard, in particular, to the prediction that the contribution of bond breaking to the intrinsic barrier is one-fourth of the bond dissociation energy. This task is the easiest in the case of benzyl chloride and bromide for which thermochemical data exist that allow the estimation of the standard potential of the $\text{PhCH}_2\text{X}/\text{PhCH}_2^* + \text{X}^-$ couple. The results of the comparison between theoretical predictions and experimental data are shown in Table II.

We start from the estimation of the standard potential E^0 versus the aqueous saturated calomel electrode in each solvent (see ref 4a and references cited therein):

$$\begin{aligned} E^0 &= \Delta E_{\text{SHE} \rightarrow \text{SCE}}^{\text{solvent}} + G_{\text{RX}}^{\text{f,solvent}} - G_{\text{R}^*}^{\text{f,solvent}} - G_{\text{X}^-}^{\text{f,solvent}} \\ &= \Delta E_{\text{SHE} \rightarrow \text{SCE}}^{\text{solvent}} + G_{\text{RX}}^{\text{f,gas}} - G_{\text{R}^*}^{\text{f,gas}} - G_{\text{X}^-}^{\text{f,solvent}} + \Delta G_{\text{RX/R}^*}^0 \end{aligned}$$

(24) Since the peak potential is shifted positively to the standard potential, α should be larger than 0.5, and thus the positive shift would be even less. Even taking for α the low values observed experimentally the same conclusion would be reached.

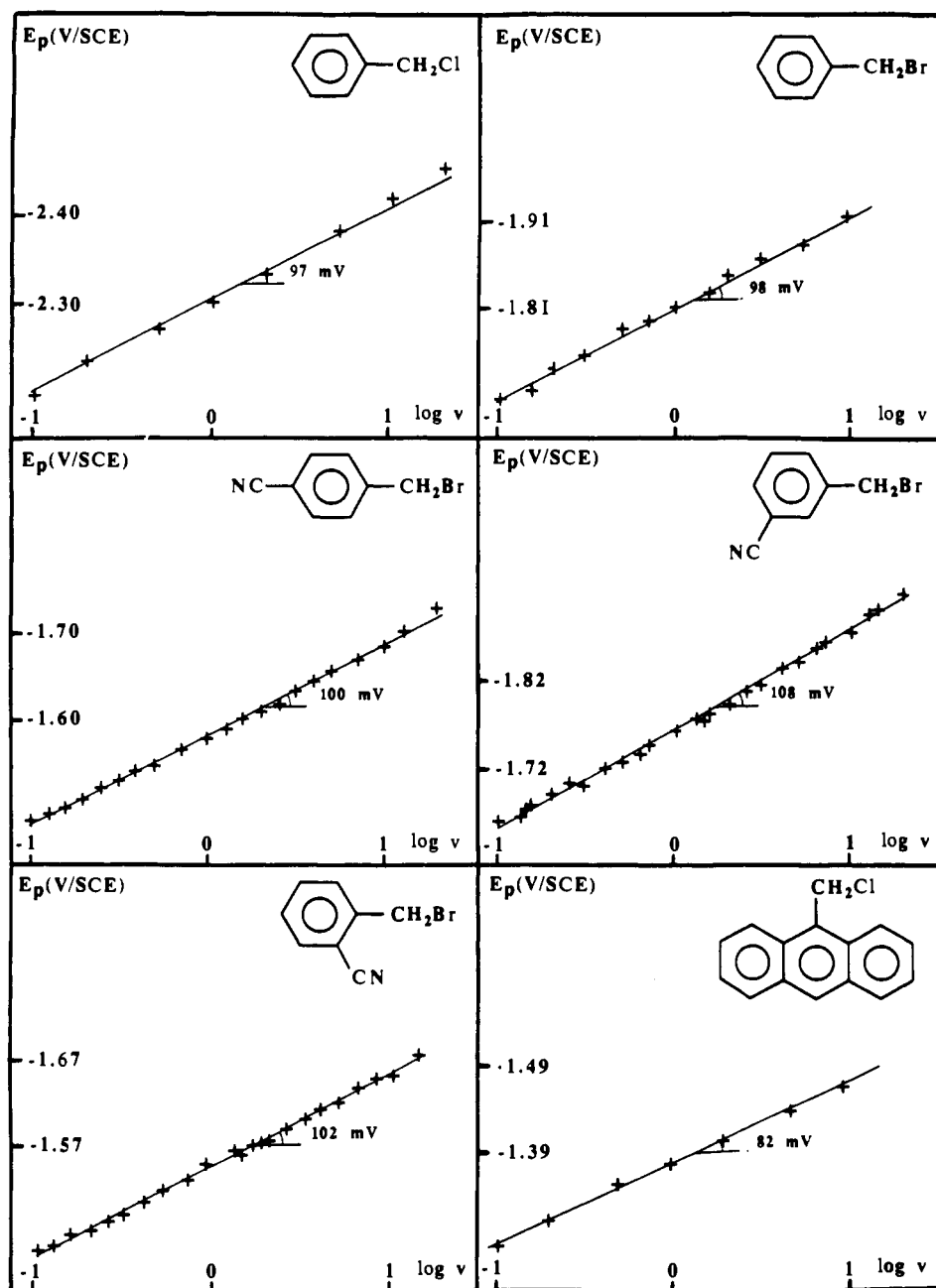
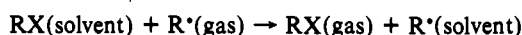


Figure 5. Cyclic voltammetry of benzyl chloride, benzyl bromide, 4-, 3-, and 2-cyanobenzyl bromides and 9-anthracenylmethyl chloride in DMF + 0.1 M *n*-Bu₄NBF₄ at a glassy carbon electrode. Variations of the peak potential of the reductive cleavage wave with the scan rate. Temperature: 25 °C. With the cyanobenzyl bromides 50 mM phenol was added to the solution.

(where the potentials are expressed in volts and the free energies in eV, RX:PhCH₂X, R*:PhCH₂*). $\Delta E_{\text{SHE} \rightarrow \text{SCE}}^{0, \text{solvent}}$ is the potential shift when passing from the standard hydrogen electrode in the solvent to the aqueous SCE. It is equal to -0.183 V in DMF and -0.255 V in CH₃CN.^{25a,b} $G_{\text{RX}}^{\text{f, gas}}$ and $G_{\text{R}^*}^{\text{f, gas}}$ are the Gibbs free energies of formation of RX and R* in the gas phase. They are equal to 1.022 (PhCH₂Cl), 1.266 (PhCH₂Br), and 2.484 (PhCH₂*) eV.^{25c} The Gibbs free energy of formation of the halides ions in the particular solvent $G_{\text{X}^-}^{\text{f, solvent}}$ is equal to -0.885 (Cl⁻) and -0.766 (Br⁻) eV in DMF and to -0.923 (Cl⁻) and -0.748 (Br⁻) eV in CH₃CN.^{25b,d} There are two ways of estimating the standard Gibbs free energy $\Delta G_{\text{RX/R}^*}^0$ of the reaction:



One is to simply neglect it. The other consists in assuming that it is the same, in the present solvents and in water, as for the corresponding methyl halides and that the Gibbs free energy of transfer of CH₃* from gas phase to water is the same as that of CH₄. It then follows^{25e} that $\Delta G_{\text{RX/R}^*}^0 = 0.112$ and 0.121 eV for

Cl and Br, respectively. The ensuing values of $E_{\text{RX/R}^*}^0$ are listed in Table II.

Once E^0 is known, the second step of the comparison between theory and experiment consists in estimating the intrinsic barrier

(25) (a) Cox, B. G.; Hedvig, G. R.; Parker, A. J.; Watts, D. W. *Aust. J. Chem.* 1974, 27, 477. (b) Geske, D. H.; Ragle, M. A.; Bambeneck, J. L.; Balch, A. L. *J. Am. Chem. Soc.* 1964, 86, 987. (c) Benson, S. W. *Thermodynamical Kinetics*, 2nd ed.; Wiley: New York, 1976. (d) Wagman, D. D.; Evans, W. H.; Parker, V. B.; Schumm, R. H.; Halow, I.; Bailey, S. M.; Churney, K. L.; Nuttal, R. L. *J. Phys. Chem. Ref. Data* 1982, 11, Suppl. 2. (e) Hush, N. S. *Z. Electrochem.* 1957, 61, 734. (f) *Handbook of Chemistry and Physics*; 52nd ed.; CRC: Cleveland, OH, 1972, p F171. (g) When $\Delta G_{\text{RX/R}^*}^0$ is neglected, D is taken from the gas phase data^{25b,e} implying that we neglect the variation of the enthalpy of formation of X* from the gas phase to the solvent. When $\Delta G_{\text{RX/R}^*}^0 \neq 0$ and estimated according to the second procedure, we also neglect this variation and, in addition, assume that the variation of the difference between the formation enthalpies of RX and R* upon passing from the gas phase to the solvent is the same as the variation of the difference between the free enthalpies, i.e., $\Delta G_{\text{RX/R}^*}^0$. This given rise to slightly different values of D ($D = D_{\text{gas}} + \Delta G_{\text{RX/R}^*}^0$) for both PhCH₂Cl and PhCH₂Br (Table II).

Table II. Comparison between the Predictions of the Theory of Dissociative Electron Transfer and the Experimental Data for the Cyclic Voltammetric Reductive Cleavage of Benzyl Chloride and Bromide^a

		compound			
		PhCH ₂ Cl		PhCH ₂ Br	
E_p^b	0.1 V/s	-2.21	-1.71		
	1.0 V/s	-2.30	-1.82		
	10.0 V/s	-2.41	-1.94		
ϕ_r^b	0.1 V/s	-0.08 ₉	-0.07 ₈		
	1.0 V/s	-0.09 ₁	-0.08 ₀		
	10.0 V/s	-0.09 ₄	-0.08 ₂		
$Z(RT/FvD)^{1/2}$	0.1 V/s	8.9×10^5	7.7×10^5		
	1.0 V/s	2.8×10^5	2.4×10^5		
	10.0 V/s	8.9×10^4	7.7×10^4		
ΔG^\ddagger^d	0.1 V/s	0.34 ₇	0.34 ₂		
	1.0 V/s	0.31 ₈	0.31 ₃		
	10.0 V/s	0.28 ₉	0.28 ₅		
E^0^b	$\Delta G_{RX/R}^\ddagger^d$	0	0.11 ₂	0	0.12 ₁
		-0.76 ₀	-0.87 ₂	-0.63 ₅	-0.75 ₆
ΔG_0^\ddagger (exp ^{al}) ^d	0.1 V/s	0.89 ₉	0.85 ₈	0.75 ₉	0.71 ₃
	1.0 V/s	0.89 ₇	0.85 ₆	0.76 ₆	0.72 ₁
	10.0 V/s	0.89 ₉	0.86 ₀	0.77 ₆	0.73 ₁
	av	0.89 ₈	0.85 ₈	0.76 ₇	0.72 ₂
a_x, a_{RX}, a	e	1.81, 3.58, 2.70	1.96, 3.61, 2.86		
	λ_0	0.76 ₇	0.72 ₉		
D	d, f	2.99	3.10	2.30	2.42
	ΔG_0^\ddagger (theor)	d	0.93 ₉	0.96 ₇	0.75 ₇
α (pred)	0.1 V/s	0.31 ₁	0.31 ₈	0.33 ₆	0.34 ₆
	1.0 V/s	0.29 ₈	0.30 ₃	0.32 ₀	0.32 ₉
	10.0 V/s	0.28 ₄	0.29 ₀	0.30 ₃	0.31 ₁
	av	0.29 ₇	0.30 ₄	0.32 ₀	0.32 ₉
α (theor)	0.1 V/s	0.31 ₉	0.33 ₉	0.33 ₅	0.36 ₁
	1.0 V/s	0.30 ₇	0.32 ₇	0.31 ₈	0.34 ₄
	10.0 V/s	0.29 ₃	0.31 ₃	0.29 ₈	0.32 ₅
	av	0.30 ₆	0.32 ₆	0.31 ₇	0.34 ₃
α (exp ^{al}) ^g	0.1 V/s	0.30 ₈	0.34 ₁		
	1.0 V/s	0.31 ₈	0.34 ₁		
	10.0 V/s	0.28 ₁	0.29 ₈		
	av	0.30 ₄	0.31 ₅		

^a In DMF + 0.1 M *n*-Bu₄NBF₄, at a glassy carbon electrode at 25 °C. ^b In V vs SCE. ^c $D = 10^{-5}$ cm²·s⁻¹, $Z = (RT/2\pi M)^{1/2} = 5.6$ and 4.8×10^3 cm²·s⁻¹ for PhCH₂Cl and PhCH₂Br respectively. ^d In eV. ^e In Å. ^f From literature thermochemical data (see text). ^g The α value at each scan rate is derived from $E_{p/2} - E_p$ and the average also contains the value derived from $\partial E_p / \partial \log v$.

free energy, ΔG_0^\ddagger from the experimental data using the quadratic relationship (1) which is expected to govern the kinetics of the electrochemical dissociative electron transfer. Given the scan rate, ΔG_0^\ddagger may be derived from the determination of the peak potential, E_p , of the irreversible cyclic voltammetry wave according to the following procedure. For an electrochemical reaction, eq 1 becomes for any electrode potential, E :

$$\Delta G^\ddagger = \Delta G_0^\ddagger \left(1 + \frac{E - E^0 - \phi_r}{4\Delta G_0^\ddagger} \right)^2 \quad (5)$$

(expressing the potential in volts and the free energies in eV) where ϕ_r is the potential difference between the reaction site and the solution. The reaction site is usually assumed to be located in the outer Helmholtz plane.^{26a} At a mercury electrode, in DMF with *n*-Bu₄N⁺ as supporting electrolyte cation, we see from previously reported data that the potential difference between the

outer Helmholtz plane and the solution varies with the electrode potential, E , in the range of interest for the present experiments, according to^{26b}

$$\phi_r = 0.022E - 0.040 \quad (6)$$

We assume that ϕ_r is close to the same value in the case of a glassy carbon electrode as used here. The potential dependent heterogeneous rate constant, $k(E)$, is related to the activation free energy, ΔG^\ddagger , by the following equation:

$$k(E) = Z \exp(-F\Delta G^\ddagger / RT) \quad (7)$$

(still expressing the free energies in eV) where Z , the heterogeneous collision frequency can be obtained from

$$Z = (RT/2\pi M)^{1/2} \quad (8)$$

(M , molar mass). The current density, i , flowing through the electrode is thus

$$i = Fk(E)C_0$$

(C_0 ; surface concentration of RX). Extending the classical treatment based on the linear Butler-Volmer equation,^{18b} to the present quadratic activation-driving force relationship, one obtains the following dimensionless expression of the cyclic voltammogram:^{8a}

$$\frac{\psi}{\Lambda^0} \exp \left[\frac{\epsilon}{4} \left(1 - \frac{\xi}{\epsilon} \right)^2 \right] = 1 - \frac{1}{\pi^{1/2}} \int_{-\infty}^{\xi} \frac{\psi(\eta)}{(\xi - \eta)^{1/2}} d\eta$$

where ψ is related to the current density by $\psi = i/FC^0D^{1/2}(Fv/RT)^{1/2}$ (see footnote 22 for definition of symbols), ξ to the difference between the electrode potential E and the standard potential by $\xi = -(F/RT)(E - E^0)$, Λ^0 to the electrochemical collision frequency Z by $\Lambda^0 = Z/(FvD/RT)^{1/2}$, and $\epsilon = 4\Delta G_0^\ddagger/RT$ is directly related to the intrinsic barrier free energy ΔG_0^\ddagger that we seek to derive from the voltammogram. The relationship between the value of ξ at the peak, $\xi_p = -(F/RT)(E_p - E^0)$, and the value of ϵ may be computed by resolution of the above integral equation using standard numerical techniques,^{18b} for each value of Z , v , and E^0 . Thus, given the scan rate, ξ_p can be obtained from the measurement of the peak potential E_p and from the value of E^0 as estimated previously. The value of ϵ and therefore that of ΔG_0^\ddagger ensue.^{26c} There is however an approximate and simpler way for deriving ΔG_0^\ddagger from the experimental E_p data that consists in linearizing eq 5 within the small range of electrode potential separating the foot from the peak of the cyclic voltammetric wave at a given scan rate. As shown earlier,^{1b,c,4a,27} the value of ΔG^\ddagger at the peak may be obtained from

$$\Delta G^\ddagger = \frac{RT}{F} \ln \left[Z \left(\frac{RT}{\alpha FvD} \right)^{1/2} \right] - 0.78 \frac{RT}{F} \quad (9)$$

and thus ΔG_0^\ddagger derives from the resolution of eq 5 as

$$\Delta G_0^\ddagger = \frac{1}{4} \{ [(E_p - E^0 - \phi_r - 2\Delta G^\ddagger)^2 - (E_p - E^0 - \phi_r)^2]^{1/2} - (E_p - E^0 - \phi_r - 2\Delta G^\ddagger) \} \quad (10)$$

Test calculations on several examples showed that the results are practically the same as those obtained by more rigorous method described above within ca. 1 meV.

The transfer coefficient α may then be estimated from the adaptation of eq 2 to the electrochemical cyclic voltammetric conditions:

$$\alpha = 0.5 \left(1 + \frac{E_p - E^0 - \phi_r}{4\Delta G_0^\ddagger} \right) \quad (11)$$

(26) (a) Delahay, P. *Double Layer and Electrode Kinetics*; Wiley: New York, 1965. (b) Kojima, H.; Bard, A. J. *Am. Chem. Soc.* **1975**, *97*, 6317. (c) The diffusion coefficient D is taken as equal to 10^{-5} cm²·s⁻¹ for both compounds. $Z = 5.610^3$ and 4.810^3 cm²·s⁻¹ for PhCH₂Cl and PhCH₂Br, respectively.

(27) (a) Lexa, D.; Savéant, J.-M.; Su, K. B.; Wang, D. L. *J. Am. Chem. Soc.* **1987**, *109*, 6464. (b) Andrieux, C. P.; Savéant, J.-M. *J. Electroanal. Chem.* **1989**, *267*, 15. (c) Lexa, D.; Savéant, J.-M.; Schäfer, H. J.; Su, K. B.; Vering, B.; Wang, D. L. *J. Am. Chem. Soc.* **1990**, *112*, 6162.

A value of α was required in eq 9 to start the preceding determination of ΔG_0^\ddagger . We used the experimentally determined value as the starting value and then, in a rapidly converging iteration procedure, the value derived from eq 11 (convergence is reached with an excellent precision after two loops).

The comparison between the values of α thus obtained, that we designate in the table as α (pred), and the experimental values provide an experimental test of the quadraticity of the activation-driving force relationship (eqs 1 and 5). α (pred) decreases upon raising the scan rate as a reflection of this quadraticity. We see that there is the same trend in the experimental values derived from the peak width. We also note that the average values of α (exp^{al}) over the whole range of scan rates are clearly below 0.5 and are in good agreement with the average values of α (pred). This observation is also consistent with the quadratic character of the activation-driving force relationship. The reason that the transfer coefficient is distinctly below 0.5 thus appears as a consequence of the fact that the reduction potential is much negative to the standard potential. This determination of ΔG_0^\ddagger has been carried out in each case for three typical scan rates, 0.1, 1.0, and 10 V·s⁻¹ as shown in Table II. The ensuing values of ΔG_0^\ddagger (exp^{al}) are practically the same for each scan rate.

The theory of dissociative electron transfer⁴ predicts that the intrinsic barrier free energy is the sum of a solvent reorganization term and of a contribution of bond breaking equal to one-fourth of the bond dissociation energy, D :

$$\Delta G_0^\ddagger = \frac{D}{4} + \frac{\lambda_0}{4} \quad (12)$$

with, according to a Marcus-like estimate of solvent reorganization:

$$\lambda_0 = \left(\frac{1}{D_{op}} - \frac{1}{D_S} \right) \frac{e_0^2}{4a} \quad (13)$$

and with a Hush-like estimate

$$\lambda_0 = \left(\frac{1}{D_{op}} - \frac{1}{D_S} \right) \frac{e_0^2}{2a} \quad (14)$$

D_{op} and D_S are the optic and static dielectric constants of the solvent respectively, a is the radius of the hard sphere equivalent to the reactant and products, and e_0 the charge of the electron.

Previous investigation of the electrochemical reduction in DMF, with $n\text{-Bu}_4\text{N}^+$ as supporting electrolyte cation, of an extended series of aromatic molecules giving rise to a stable anion radical has shown that the intrinsic barrier is roughly proportional to the inverse of the hard sphere equivalent radius of the molecule, a .^{26b} The proportionality coefficient falls in between the predictions of the Marcus and Hush models. Since the reaction is a good approximation of an outer-sphere electron transfer with, in view the robustness of the aromatic framework, little or no inner-sphere reorganization, these results may serve for estimating the solvent reorganization factors from the size of the molecule:

$$\lambda_0 \text{ (eV)} = 2.08/a \text{ (\AA)} \quad (15)$$

The estimation of a in the present case is not as straightforward as in the outer-sphere case. What is necessary to estimate here is the reorganization of the solvent around the halogen atom, when its charge passes from 0 to -1, partially hindered by the organic portion of the molecule. Previous estimations^{4a} have used the arithmetic mean of the halogen radius, a_X , and of the radius of the sphere equivalent to the whole molecule, a_{RX} , itself derived from the molar mass, M , and the density, ρ :

$$a_{RX} = (3M/4N_A\rho)^{1/3} \quad (16)$$

The following equation

$$a = \frac{a_X(2a_{RX} - a_X)}{a_{RX}} \quad (17)$$

probably gives a more realistic estimation and was used in the following.

Using the values of λ_0 thus estimated and values of the bond dissociation energies from the literature,^{25c,f} one obtains^{25g} the theoretical values of the intrinsic barrier, ΔG_0^\ddagger (theor), listed in Table II.

We see that there is a quite satisfactory agreement between the predictions of the theory in terms of intrinsic barrier free energy and the experimental values. As seen in Table II, the agreement is distinctly better when E^0 and D are estimated directly from the gas phase thermochemical data concerning RX and R^+ than when $\Delta G_{RX/R^+}^0$ is calculated from the second procedure.

Regarding the transfer coefficient, there is also a good agreement between theory and experimental data as can be seen in Table II where the average experimental values from Table I are compared to the values obtained from eq 11 using for ΔG_0^\ddagger the theoretical value derived from eq 12 (The values of α (theor) thus obtained, reported in Table II, are the averages of the three values obtained for the three values of E_p , themselves corresponding to the three scan rates 0.1, 1.0, and 10 V·s⁻¹). We again see that the agreement between theory and experiment is better when $\Delta G_{RX/R^+}^0$ is neglected in the estimation of E^0 and D .

Derivation of Unknown Bond Dissociation Energies from Peak Potential Data. Since the validity of the dissociative electron transfer theory is verified so well in the case of benzyl chloride and bromide, we may assume it is also valid in the case of the cyano- and carbomethoxybenzyl bromides and of anthracenylmethyl chloride and therefore use it to estimate the C-X bond dissociation energy of these compounds from the values of their peak potentials in cyclic voltammetry. The principle of this estimation is as follows. The standard potential of the $RX/R^+ + X^-$ couple, E^0 , may be decomposed as

$$E^0 = -D - T(\bar{S}_{RX} - \bar{S}_{R^+} - \bar{S}_{X^-}) + E_{X^*/X^-}^0$$

where D is the C-X bond dissociation energy, E_{X^*/X^-}^0 the standard potential of the X^*/X^- couple and \bar{S}_{RX} , \bar{S}_{R^+} , and \bar{S}_{X^-} the partial molar entropies of the subscript species. When comparing, for each X , one RX in the series to PhCH_2X , E_{X^*/X^-}^0 and \bar{S}_{X^-} do not change, whereas the variation in $\bar{S}_{RX} - \bar{S}_{R^+}$ is likely to be negligibly small. Thus, with a good approximation

$$E^0 = (E_{\text{PhCH}_2X}^0 + D_{\text{PhCH}_2X}) - D$$

Thus, given the halogen, the following relationship between the standard potential and the bond dissociation energy applies for all compounds in the series

$$E^0 = -D + C \quad (18)$$

C being obtained from the unsubstituted benzyl halides values:

$$C = E_{\text{PhCH}_2X}^0 + D_{\text{PhCH}_2X}$$

Treating the cyclic voltammograms along the same linearization procedure as described precedingly, we may thus derive the value of D from the experimental value of the peak potential, E_p , according to the following procedure. The activation free energy at the peak potential, ΔG^\ddagger , is obtained again from eq 9. Application of the activation-driving force relationship 5 leads to

$$\Delta G^\ddagger = \frac{D + \lambda_0}{4} \left(1 + \frac{E_p - E^0 - \phi_r}{D + \lambda_0} \right)^2 \quad (19)$$

and thus, taking eq 18 into account

$$D = \frac{1}{2} \{ [(\lambda_0 + E_p - C - \phi_r - \Delta G^\ddagger)^2 + 4\lambda_0\Delta G^\ddagger - (\lambda_0 + E_p - C - \phi_r)^2]^{1/2} - (\lambda_0 + E_p - C - \phi_r - \Delta G^\ddagger) \} \quad (20)$$

λ_0 is obtained from by means of eq 15, a being estimated using eq 16 and 17.

The values of D thus derived from the experimental E_p values are listed in Table III. Rather than absolute values deriving from the application of eq 20, we have reported the difference between the bond dissociation energies of the considered compound and

the corresponding benzyl bromide or chloride since the calculations have taken, through the value of C , as pivotal quantities the thermochemical data pertaining to these two compounds.

As seen from Table III there are significant differences in bond dissociation energies between the cyano- and carbomethoxybenzyl bromides and benzyl bromide as well as between anthracenylmethyl chloride and benzyl chloride. Since $Z(RT/F\lambda D)^{1/2}$ and λ^0 do not vary much in the whole series, the essential reason that the reduction potential, at each scan rate, varies from one compound to the other derives from the variation of the bond dissociation energy through the corresponding variations of E^0 and ΔG_0^\ddagger .

The bond dissociation energies of a series of 4-substituted benzyl bromides have been recently determined using photoacoustic calorimetry,⁹ i.e., a technique entirely independent from the procedures that led us to the values gathered in Table III. We see that for 4-cyanobenzyl bromide there is a fair agreement between the photoacoustic calorimetry value (0.216 eV with a gap between the extreme values determined of 77 meV) and our value (0.149 eV). Although the difference is not far from the magnitude of the experimental uncertainty, our value appears smaller than the photoacoustic calorimetric value. This might be related to the fact that the latter was obtained in a different and less polar medium, a 3:1 diethylsilane-benzene mixture, than ours (DMF + 50 mM benzoic acid). The trend that the bond dissociation energies are weakened by electron-withdrawing substituent on the benzene ring (assigned mostly to changes in the formation enthalpy of the starting bromide rather than of the radical⁹) is thus confirmed. As expected along these lines, the ΔD for the ortho-substituted cyano derivative is close to that of the para-substituted derivative and distinctly lower for the metal-substituted derivative. There is a much larger weakening of the bond when passing from benzyl to anthracenylmethyl chloride.

We thus see that the difference in peak potentials may be utilized to obtain an estimate of the difference between the bond dissociation energies of two compounds bearing the same halogen and thus obtain the bond dissociation energy of an unknown compound from that of a compound for which thermochemical data are available from other source. The procedure we have used may be made simpler and quicker by neglecting the differences in Z , D , and λ_0 for two compounds of similar size and neglecting the quadratic character of the activation-driving force relationship in the case where the peak potentials at the same scan rate are not too distant. Under such conditions

$$\Delta\Delta G^\ddagger = 0$$

and thus

$$\Delta D = -\frac{2}{3}\Delta E_p \quad (21)$$

We see from Table III that the results of this quick estimation are not too different from those of the more rigorous procedure used previously.

The quadratic character of the activation-driving force relationship (eq 1) may nevertheless be tested in this series of five compounds as done previously with benzyl chloride and bromide. In this connection, Table III contains a comparison between the experimental values of the transfer coefficient α ($\exp^{2\lambda}$) and the values of α (pred) obtained by injecting in eq 11 the values of ΔG_0^\ddagger derived from the experimental values of E_p . It is seen that the agreement is again satisfactory. There is in this case too, a distinct trend for the experimental values to decrease upon raising the scan rate, i.e., upon increasing the driving force as expected from the quadratic character of the activation-driving force relationship.

We have also listed in Table III the values of E^0 and ΔG_0^\ddagger that are predicted on the basis of the preceding estimation of D using eqs 18 and 12, respectively.

Factors Governing the Passage from the Concerted to the Stepwise Mechanism. The examples described above have demonstrated that, even within the same family of compounds, the reductive cleavage may follow one or the other mechanism. At the level of driving forces, the occurrence of one or the other mechanism is governed by the potential difference

$$E_{RX/R^{\cdot+}X^-}^0 - E_{RX/RX^{\cdot-}}^0 = -D - T(\bar{S}_{RX} - \bar{S}_R - \bar{S}_{X^{\cdot-}}) + E_{X^{\cdot-}/X^-}^0 - E_{RX/RX^{\cdot-}}^0$$

the more positive $E_{RX/R^{\cdot+}X^-}^0 - E_{RX/RX^{\cdot-}}^0$ the larger the preference for the concerted mechanism on thermodynamical grounds. Given the departing group, the preference for the concerted mechanism will be enhanced by small values of the R-X bond dissociation energy and by more and more negative values of the standard potential for the formation of the anion radical, $E_{RX/RX^{\cdot-}}^0$. $E_{RX/RX^{\cdot-}}^0$ is a measure of the free energy of the unpaired electron residing temporarily in an accessible unoccupied orbital of the RX molecule; here the π^* orbital is on the aromatic moiety, before being transferred to the σ^* C-X orbital concertedly with the cleavage of the C-X bond. In addition to this, one has to take account of the fact that different activation barriers are to be overcome for generating the anion radical on one hand and for triggering the concerted reductive cleavage on the other. As results from the data reported above, the intrinsic barrier for the dissociative electron transfer is larger than that for the outer-sphere formation of $RX^{\cdot-}$ resulting in a kinetic disadvantage of the first reaction over the second for comparable driving forces.

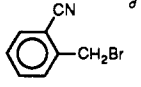
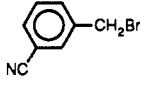
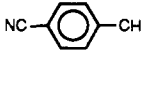
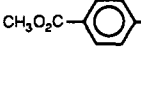
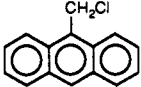
Within this framework the fact that the nitro-substituted derivatives follow the stepwise mechanism whereas all the others follow the concerted mechanism is essentially a reflection of the π^* orbital on the aromatic group being much lower in energy in the first case than in the second. There is a definite trend for the bond dissociation energy to decrease as the substituent becomes more and more electron-withdrawing. This should favor the concerted mechanism in the case of the nitro-substituted derivatives. However this effect is small (of the order of 150 meV when passing from unsubstituted to CN-substituted derivatives and only slightly more for nitro-substituted derivatives), whereas the change in $E_{RX/RX^{\cdot-}}^0$ is considerably larger (of the order of 1.3 V from 4-nitro- to 4-cyanobenzyl bromide, for example).

As seen in Figure 1, it is conceivable that a transition between the concerted and stepwise mechanisms could be observed with the same substrate upon varying the driving force of the reductive cleavage by means of a variation of the scan rate in the present case: low scan rates (low driving forces) should favor the concerted mechanism and high scan rates (high driving forces) the stepwise mechanism. However, in the present series of compounds, the π^* orbital is too low in the nitro-substituted derivatives and too high in the CN-substituted derivatives for the passage to the concerted mechanism in the first case (upon decreasing the scan rate) and to the stepwise mechanism in the second (upon raising the scan rate) to be observed in the accessible range of scan rates. The observation of the transition between the two mechanisms requires a special design of the compound to be tested. Preliminary results seem to indicate that such a transition is observed with 1,2-dibromo-3-(4-cyano- or 4-carbomethoxyphenyl)propanes.²⁸

In the same vein, there is the striking difference between the electrochemical reductive cleavage of the 3-cyanobenzyl bromide in DMF that we have observed here and its previously reported reductive cleavage by pulse radiolysis in water.^{12d} The anion radical is observed in pulse radiolysis in water^{12d} with a decay rate constant of $1.3 \times 10^7 \text{ s}^{-1}$, whereas, as discussed before, electron transfer and bond breaking are concerted during the electrochemical reduction in DMF. One reason for this difference in behavior may be that the driving force of the reaction is much larger in the first case than in the second: the standard potential of the solvated electron in water has been estimated as ca. -3.11 V vs SCE,^{29a} whereas the cyclic voltammetric reduction takes place under much milder conditions since the peak potential varies between -1.53 V vs SCE at 0.1 V s⁻¹ and -1.74 V vs SCE at 10 V s⁻¹. One additional reason may be that the anion radical is likely to be less kinetically stable in DMF than in water. In this connection we note that, at room temperature, the lifetime of the anion radical of 4-nitrobenzyl chloride in water (250 μs) is longer by three orders of magnitude than that in DMF (0.25 μs).^{29b}

(28) Andrieux, C. P.; Le Gorande, A.; Savéant, J.-M., manuscript in preparation.

Table III. Determination of the Bond Dissociation Energy Increments from the Cyclic Voltammetric Peak Potential and Test of the Quadratic Character of the Activation-Driving Force Relationship^a

compound	a_X (Å) a_{RX} (Å) a (Å) λ_0 (eV)	C (eV) $Z \times 10^{-3}$ (cm/s)	scan rate (V/s)	$-E_p$ (V vs SCE)	$-\phi_r$ (mV)	ΔG^* (meV)	$-\Delta D^b$ (meV)	$-E^0$ (V vs SCE)	ΔG_0^* (meV)	α pred	α exp ^{alc}
	1.96	1.66 ₅	0.1	1.44	7 ₂	34 ₁	15 ₆ (18 ₀)	0.47 ₉	71 ₇	0.34 ₅	0.36 ₇
	3.69		1.0	1.53	7 ₄	31 ₂	15 ₅ (19 ₃)	0.48 ₀	71 ₈	0.33 ₀	0.31 ₈
	2.88	4.63	10	1.63	7 ₆	28 ₃	15 ₁ (20 ₇)	0.48 ₄	71 ₈	0.31 ₄	0.28 ₉
	0.724		av				15 ₄ (19 ₃)	0.48 ₁	71 ₈	0.33 ₀	0.31 ₅
	1.96	1.66 ₅	0.1	1.62	7 ₆	34 ₁	5 ₀ (6 ₀)	0.58 ₄	74 ₄	0.33 ₉	0.34 ₁
	3.69		1.0	1.72	7 ₈	31 ₂	4 ₄ (6 ₇)	0.59 ₁	74 ₅	0.32 ₄	0.31 ₈
	2.88	4.63	10	1.83	8 ₁	28 ₃	3 ₄ (7 ₃)	0.60 ₁	74 ₇	0.30 ₈	0.26 ₅
	0.724		av				4 ₃ (6 ₇)	0.59 ₂	74 ₅	0.32 ₄	0.29 ₃
	1.96	1.66 ₅	0.1	1.46	7 ₂	34 ₁	14 ₉ (16 ₆)	0.49 ₁	71 ₉	0.34 ₄	0.34 ₁
	3.69		1.0	1.54	7 ₄	31 ₂	14 ₉ (18 ₇)	0.48 ₆	71 ₉	0.33 ₀	0.32 ₉
	2.88	4.63	10	1.65	7 ₇	28 ₃	13 ₉ (19 ₃)	0.49 ₆	72 ₁	0.31 ₃	0.29 ₈
	0.724		av				14 ₉ (18 ₂)	0.49 ₁	72 ₀	0.32 ₉	0.33 ₂
	1.96	1.66 ₅	0.1								
	4.22		1.0								
	3.01	3.79	10	1.56	7 ₄	27 ₈	18 ₈ (25 ₃)	0.44 ₇	70 ₁	0.31 ₅	0.34 ₁
	0.693										
	1.81	2.23 ₀	0.1	1.29	6 ₈	33 ₆	59 ₉ (61 ₃)	0.16 ₁	77 ₆	0.32 ₉	0.39 ₈
	4.22		1.0	1.36	7 ₀	30 ₇	61 ₂ (62 ₇)	0.14 ₉	77 ₃	0.31 ₅	0.38 ₂
	2.84	3.75	10	1.44	7 ₁	27 ₈	62 ₁ (64 ₇)	0.13 ₉	77 ₀	0.30 ₁	0.36 ₇
	0.714						61 ₁ (62 ₉)	0.15 ₀	77 ₃	0.31 ₅	0.37 ₂

^aIn DMF + 0.1 M *n*-Bu₄NBF₄ at a glassy carbon electrode at 25 °C. ^bBetween parentheses: approximate estimation from eq 21 (see text). ^cThe indicated average value is the average between the average of the values derived from $E_{p/2} - E_p$ and the value derived from $\partial E_p / \partial \log v$. ^dIn the presence of 50 mM benzoic acid.

Conclusions

The main conclusions that emerge from the above results are as follows. There is a striking change in the mechanism of reductive cleavage of arylmethyl halides when one passes from the ring-substituted nitro derivatives to the other compounds in the series. With the nitro-substituted benzyl chlorides and bromides, the mechanism involves the formation of the anion radical as an intermediate. When slightly less electron-withdrawing substituents, such as nitrile or ester groups, are involved, the reaction occurs via a concerted electron transfer-bond breaking mechanism. This is also observed with the unsubstituted benzyl chloride and bromide as well as with 9-anthracenylmethyl chloride. Given the nucleofugal group, the main factor that governs the occurrence of one rather than the other mechanism in the series appears to be the energy of the π^* orbital: the higher this energy, the more pronounced the tendency for the concerted mechanism to be followed and vice versa.

In the cases where the concerted mechanism prevails, the main parameter governing the reduction thermodynamics and kinetics is the dissociation energy of the bond undergoing cleavage in the reaction. In this connection, the predictions of the recently developed theory of dissociative electron transfer are in excellent agreement with the experimental data for what regards both the quadratic character of the action-driving force relationship and the magnitude of the intrinsic barriers based on independently known values of the bond dissociation energies. The difference

in the cyclic voltammetric peak potentials of two compounds bearing the same nucleofugal group may thus serve as a basis for estimation of the difference between their bond dissociation energies. If the peak potentials are not too far apart, a quick and simple approximate procedure may be used that predicts that the difference in bond dissociation energies is two-thirds of the distance between the peak potentials at the same scan rate, taking into account that the more negative the peak potential, the larger the bond dissociation energy.

Experimental Section

Chemical. Acetonitrile (Mercks Uvasol) was used as received and DMF (Merck) was vacuum distilled before use. The supporting electrolyte, *n*-Bu₄NBF₄ (Fluka, puriss), was used as received. The arylmethyl halides investigated in this study were from commercial origin (Fluka, Aldrich).

Instrumentation. The conventional microelectrodes used in this work were glassy carbon, gold or platinum disks of 1–3-mm diameter. They were carefully polished and ultrasonically rinsed with ethanol before each run. The ultramicroelectrodes used in the high scan rate experiments were gold or platinum disks of 5- and 17- μ m diameter polished in the same way before use. The counterelectrode was a platinum wire and the reference electrode an aqueous SCE electrode or a Cd(Hg)/CdCl₂/NaCl/DMF electrode.^{30a} The latter electrode was preferred for the systematic determination of peak potentials and peak widths for a series of scan rates.

The potentiostat equipped with a positive feedback compensation and current measurer used at low or moderate scan rates was the same as previously described.^{30b} The instrument used with ultramicroelectrodes at high scan rate has been described elsewhere.^{30c}

Acknowledgment. We are indebted to Dr. D. D. M. Wayner (National Research Council of Canada, Ottawa) for the kind communication of his photoacoustic calorimetric bond dissociation energy data⁹ prior to publication.

Registry No. PhCH₂Cl, 100-44-7; PhCH₂Br, 100-39-0; 4-cyanobenzyl bromide, 17201-43-3; 3-cyanobenzyl bromide, 28188-41-2; 2-cyanobenzyl bromide, 22115-41-9; 9-anthracenylmethyl chloride, 24463-19-2; 4-nitrobenzyl chloride, 100-14-1; 4-nitrobenzyl bromide, 100-11-8; 3-nitrobenzyl chloride, 3958-57-4; 2-nitrobenzyl chloride, 612-23-7; 4-acetyloxybenzyl bromide, 52727-95-4.

(29) (a) Hart, E. J.; Anbar, M. *Hydrated Electron*; Wiley: New York, 1970. (b) The reasons of this considerable difference in lifetimes from an aprotic to a protic solvent have not been elaborated so far. We suggest the following qualitative explanation. In the anion radical a considerable portion of the negative charge is located on the oxygen atoms of the nitro group. A strong interaction of this portion of the anion radical with water molecules is thus likely. This is expected to have two main effects on the kinetics of the cleavage reaction which may be viewed as an intramolecular dissociative electron transfer.^{4b} One is to lower the energy of the π^* orbital in which the unpaired electron is mostly located and therefore to decrease the driving force of the cleavage reaction (a roughly linear correlation has been shown to exist between the cleavage activation free energy and the standard potential of the anion radical, with a slope close to 0.5, in the case of aromatic halides anion radicals^{4b}). The other effect regards solvent reorganization which ought to be large since the solvation of the NO₂⁻ group by water molecules has to be changed into a solvation of the leaving chloride ion. It is remarkable in this connection that very large preexponential factors have been found in the cleavage kinetics of nitro-substituted benzyl halide anion radicals in water^{12d} implying a positive entropy of activation.

(30) (a) Marple, L. W. *Anal. Chem.* 1967, 39, 844. Manning, C. W.; Purdy, W. C. *Anal. Chim. Acta* 1970, 51, 124. (b) Garreau, D.; Savéant, J.-M. *J. Electroanal. Chem.* 1972, 35, 309. (c) Garreau, D.; Hapiot, P.; Savéant, J.-M. *J. Electroanal. Chem.* 1989, 272, 1.